学 術
Arts and Sciences
原 著

New simple imaging method for short-axis view in cardiac MRI inferred from chest X-ray

胸部単純X線画像から推論した心臓MRIにおける新しい短軸像撮像手法の検討

FUJII Tomoki[1], USUI Hiromi[2], SATO Hisaya[1, 3], KATO Kyoichi[3, 4]

1) Showa University Hospital, Department of Radiological Technology
2) Showa University Northern Yokohama Hospital, Department of Radiological Technology
3) Showa University Graduate School of Health Sciences
4) Showa University Radiological Technology

Key words: Cardiac Magnetic Resonance Imaging, Short Axis, Chest X-rays, Coronary Computed Tomography Angiography, New simple imaging method, Reliable imaging method

【Abstract】

Cardiac Magnetic Resonance Imaging (CMRI) is often performed under respiratory standstill. Vertical Long Axis imaging (VLA) and Horizontal Long Axis imaging (HLA) are used to acquire short-axis imaging (SA) although it requires patients to hold their breath for a long time. Therefore, in some patients, the image quality in SA may be affected by repeated breath-holds. This study aims to devise a new method to acquire SA without VLA and HLA.

Initially, 116 patients who underwent Coronary Computed Tomography Angiography (CCTA) and front and lateral chest X-rays were investigated to assess the relationship between the SA angle in the CCTA images and the angle of the cardiac shadow in the X-rays for application in the new method. Then, 20 subjects were randomly selected for assessment of inter- and intra-reproducibility studies. Finally, 10 participants underwent CMRI using the new and the conventional methods for visual and objective evaluations.

A strong relation was found between the SA angle and the cardiac shadow. The measurements of the SA angle and the cardiac shadow were excellently reproducible. Compared with the conventional method, the new method proposed in this study has improved the time of respiratory standstills. It is suggested that this new method has the potential to provide a high-quality image as obtained with the conventional method.

【要 旨】

心臓シネMRIにおいて心臓短軸像を得るには，水平長軸像・垂直長軸像を用いて多くの息止めを要しながら撮像断面を決定している．そのため被検者からは，検査時間の短縮や息止め回数の減少を訴えられることが見受けられた．本研究では，胸部単純X線画像から心臓の短軸像の角度を推測し，水平長軸像・垂直長軸像を撮像せずに短軸像を得る方法（新法）を検討した．本研究の結果として，心陰影から短軸角度を推測することで，水平長軸像・垂直長軸像を撮像せずに，従来と同様の短軸像を得られることが示唆された．この新法を用いることで，短軸像を得るまでの撮像時間および息止め回数を減少させることができ，被検者の負担軽減になると考える．

1. Introduction

Cardiac Magnetic Resonance Imaging (MRI) is an indispensable examination that can diagnose cardiac function and display morphological information. Cardiac MRI is also useful in evaluating the prognosis of patients with coronary artery disease [1, 2]. Cardiac delayed contrast MRI has been used for myocardial viability diagnosis of myocardial infarction and is reported to be effective in the detection of right ventricular infarction and asymptomatic infarction [3, 4]. In addition, stress tested myocardial perfusion MRI has higher spatial resolution than single-photon emission computed tomography (SPECT), and it has been reported to enable the visualization of subendocardial ischemia clearly [5].

Cardiac cine MRI can acquire a moving image in an arbitrary direction without artifacts due to bone or air compared with ultrasonography. Currently, cardiac cine MRI is the gold standard of cardiac function diagnosis method because it can acquire left ventricular function accurately and quantitatively in most myocardial deformities and abnormalities [6]. Furthermore, quantitative analysis of the left ventricular function using cardiac cine MRI is highly reproducible [7, 8].

Cardiac cine MRI is performed under paused breathing. To obtain a short-axis cross-sectional image of the heart, the imaging section is commonly set by using the vertical long-axis section image (VLA) and horizontal long-axis section image (HLA). However, VLA and HLA imaging require the patient to stop respiration for several seconds. Therefore, the diagnosis of cardiac function analysis is affected in patients with difficulty in stopping respiration due to poor short-axis cross-sectional images. In such patients, images can

藤井 智希[1]，薄井 裕美[2]，佐藤 久弥[1, 3]，加藤 京一[3, 4]

1）昭和大学病院　放射線技術部
2）昭和大学横浜市北部病院　放射線技術部
3）昭和大学大学院　保健医療学研究科
4）学校法人昭和大学　統括放射線技術部

Received March 26, 2019; accepted March 27, 2020

be acquired for cardiac MRI using synchronous respiration imaging along with synchronous electrocardiogram imaging. However, this method is tedious for the operator and patients, as it takes longer examination time for imaging. Moreover, the short-axis cross-sectional image is acquired by the operator subjectively based on a short axis defined as the perpendicular cross-sectional images connecting the apex and the base of the heart. This subjective position setting might differ from operator to operator, thereby causing an uncertainty in the position.

This study aims to suggest a new examination method for acquiring short-axis cross-sectional images without HLA and VLA by using the cardiac shadow of the chest X-ray.

2. Methods

2.1 Materials

SOMATOM Definition AS+ (SIEMENS Co., Ltd.) was used for the CT examination, BENEO (FUJIFILM Co.) for the X-ray examination, and MAGNETOM AVANTO 1.5T (SIEMENS Co., Ltd.) for the cardiac MRI. ZIO Station2 (Amin Co.) was used as a medical image processing workstation for measuring the short-axis angle of the cardiac CT image. Synapse (FUJIFILM Co.) was used for the measurement of the short-axis angle in the X-ray image. Statistical analysis was performed using JMP 13.0 (SAS Institute Inc.).

2.2 Measurement of short axis in cardiac X-ray and CT

2.2.1 Participants

The subjects in the study were 116 patients who had underwent coronary computed tomography angiography (CCTA) and front and lateral chest X-ray examinations from January 2012 to August 2013. No criteria were set for the time interval between the chest X-ray examination and the CCTA examination. Characteristic of the 116 participants was shown in Table 1. CCTA examination have been performed in various ways, and most patients who underwent CCTA were suspected of stable work angina. Two of the 116 patients underwent CCTA for morphological assessment of dilated cardiomyopathy or cardiac tumor. Also, 14 of the 116 patients (12%) have history of Cardiac hypertrophy.

As a result of CCTA, 51 participants were confirmed at least 50% stenosis at coronary artery (15 in one-branch, 11 in two-branch, and 25 in three-branch, respectively). Also, few patients diagnosed with Kawasaki disease, dilated cardiomyopathy, and heart tumors were also included. This research was approved by the Ethics Committee at the Showa University School of Medicine.

2.2.2 Visualization of the cardiac short axis in CT

HLA and VLA images were displayed using Multi-Planar Reconstruction (MPR) from the volume CT data. A line connecting the center of the mitral valve and the apex of the heart was defined as the "short axis", which was drawn using a 3D measurement tool (Fig.1a).

2.2.3 Measurement of cardiac short-axis angle in CT imaging

The coronal section was displayed using the CT volume data. The angle "A" between the body axis and the short axis of the heart was measured. The body axis is based on the spinous processes of the thoracic vertebrae,

Table 1 Characteristic of the 116 participants who underwent CCTA

Parameters	Studied Group (N=116)	Parameters	Studied Group (N=116)	Parameters	Studied Group (N=116)
Sex		Purpose of CCTA examination		Diagnosis for CCTA*	
Male	75 (64.7%)	Stable work angina	36	Coronary Disease	51
Female	41 (35.3%)	OMI	16	Single vessel disease	15
		Chest pain	11	Double vessel disease	11
Age (years)		Exertion angina	9	Triple vessel disease	25
Mean ± SD	66.4 ± 13.7	palpitation	6	Intact vessels	65
Range	24 - 89	Heart Failure	5	Kawasaki disease	1
		Back pain	4	Dilated cardiomyopathy	1
Height (cm)		Paroxysmal artrial fibrillation	4	Cardiac tumor	1
		syncope	4		
Mean ± SD	161.8 ± 8.9	Vasospastic angina	4	History of Cardiac Hypertrophy	14
Range	140.0 - 180.0	Chronic artrial fibrillation	3		
		PVC	3		
Weight (kg)		AMI	2		
Mean ± SD	61.6 ± 14.7	Heart murmur	2		
Range	28.0 - 162.0	Scleening for operation	2		
		Chest compression	2		
Body Mass Index (kg/m^2)		Kawasaki disease	1		
Mean ± SD	23.4 ± 4.43	Dilated cardiomyopathy	1		
Range	10.0 - 50.0	Cardiac tumor	1		

Value are mean ± SD.

* Multiple selections were possible in these parameters

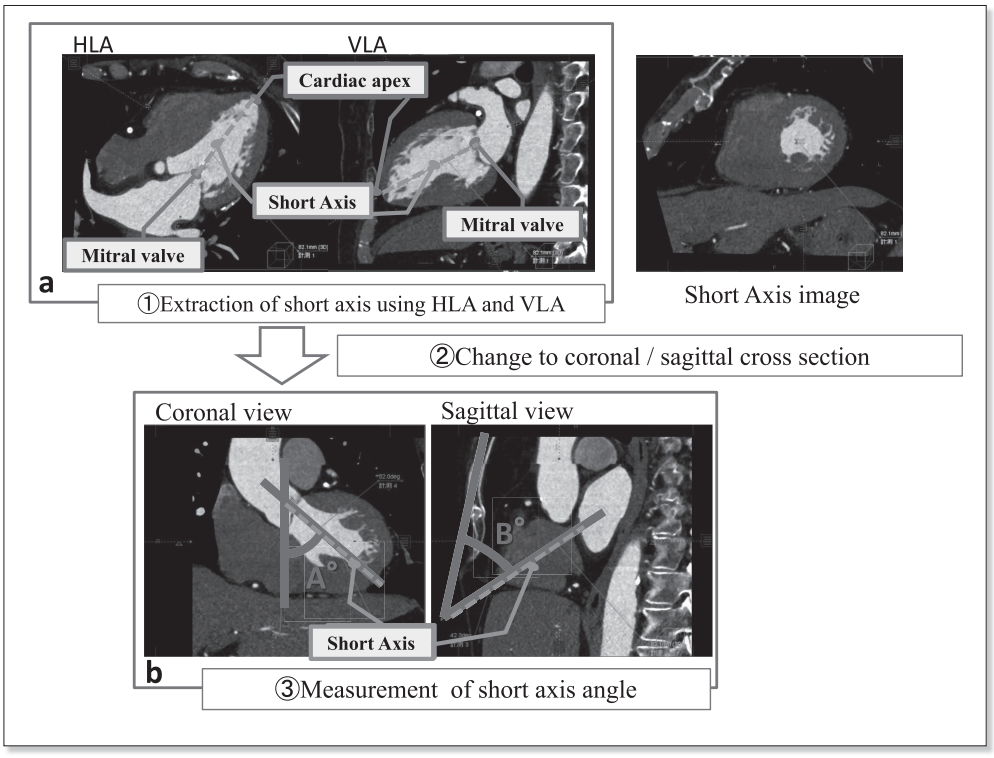

Fig.1 Extraction and measurement of cardiac short-axis angle in CT imaging

a: HLA and VLA images were displayed using Multi-Planar Reconstruction (MPR) from the volume CT data. A line connecting the center of the mitral valve and the apex of the heart was defined as the "short axis", which was drawn using a 3D measurement tool.

b: The coronal and sagittal section was displayed using the CT volume data. The angle "A" between the body axis and the short axis of the heart and the angle "B" between the sternum and the short axis of the heart were measured as the short axis angle.

and when the deformity of the thoracic vertebra is significant, it is based on the axis of the sternum.

Next, the sagittal section was displayed using the same volume data. Following this, the angle "B" between the sternum and the short axis of the heart was measured. Lateral chest X-ray examination was performed in a standing position, and the body axis depicted on the image changes according to the examined position. To evaluate the anatomical angle, we measured the angle between the sternum and the short axis of the heart (Fig.1b).

2.2.4 Measurement of cardiac shadow in chest X-ray image

Using the cardinal shadow of the XP frontal image, a cardiac lateral edge corresponding to the third and fourth bows representing the left atrium and the left ventricle were connected as the line for measurement of the angle α (expected short axis from the XP frontal image) formed by this line and the median (Fig.2a). The median is based on the spinous processes of the thoracic vertebrae; when the deformity of the thoracic vertebra is intense, it is based on the sternum axis.

Next, an XP lateral image was displayed on Synapse. From the anatomical structure, we noticed that the left atrium is the most dorsal side of the heart. Therefore, the point of the cardiac shadow located at the farthest end and the apex of the heart were connected by a line using the XP lateral image. The angle β between this line and the sternum axis (the expected short axis from the XP lateral image) was measured (Fig.2b).

2.2.5 Comparison of cardiac short axis in chest X-ray and CT

The relationship between the chest X-ray image described above and the minor axis angle of the CT was examined. We analyzed the relevancies of the angle α of the cardiac shadow in the XP frontal view and the short-axis cardiac angle A in the coronal section as well as the angle β of the cardiac shadow in the XP lateral image and the cardiac short-axis angle B in the sagittal section using the cardiac CT. The analysis was performed using Pearson's correlation of the regression line. A linear approximation formula of the regression line of angle α and angle A, and that of angle β and angle B were calculated for angle consistency.

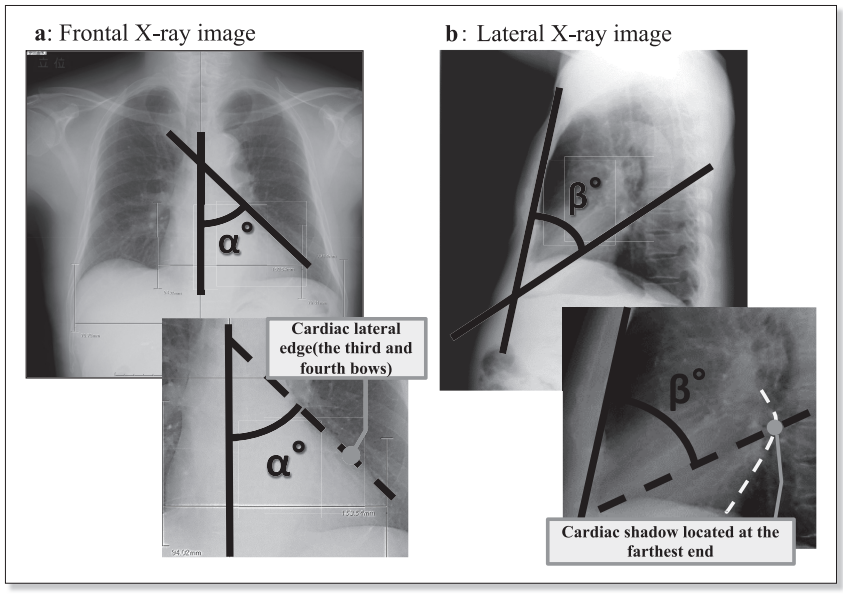

Fig.2 Measurement of cardiac shadow in chest X-ray image

a: A cardiac lateral edge corresponding to the third and fourth bows were connected as the line for measurement of the angle α formed by this line and the median in the XP frontal image.

b: The point of the cardiac shadow located at the farthest end and the apex of the heart were connected by a line using the XP lateral image. The angle β between this line and the sternum axis was measured.

2.2.6 Verification of reproducibility of measurement method

Inter-observer and intra-observer reproducibility analyses were performed by two experienced observers in 20 cases randomly extracted from the cases selected for the study. As parameters of the reliability analysis, the intraclass correlation coefficient (ICC) and the difference between the measurements of both groups as the mean difference and standard deviation of the mean difference were measured. We evaluated the ICC higher than 0.8 as "Excellent" and from 0.6 to 0.8 as "Moderate". The interval in each intra-reliability analysis was more than two weeks. The inter-reliability analysis was performed using the above-described measurement method by a radiologic technologist with 5 or more years of experience in projectional radiography and CT examination. Each result was evaluated by comparing with the underlying analysis data.

2.3 Comparison between the new method and the conventional method

Cardiac cine magnetic resonance imaging was performed on a subject by using the result obtained from the relation between the cardiac shadow and the true short-axis angle.

2.3.1 Participants

The 10 participants were volunteers who agreed to perform cardiac cine MRI examination and agreed with the purpose of this study. The participants were randomly divided into two groups to compare the conventional and new methods.

2.3.2 Examination of cardiac cine MRI with short-axis angle obtained from cardiac shadow

A localized image was taken containing three directions corresponding to the transverse, coronal, and sagittal sections so that the position and morphology of the heart could be recognized. The localized image of the coronal section was taken from a cross section in which the margin of the heart was depicted. Similarly, the localized image of the sagittal section was imaged so that the apex of the heart and its dorsal side were visualized.

Next, using the localized images of the coronal and sagittal sections, the imaging angle was adjusted to the short-axis angle based on the relation between the cardiac shadow and the true short-axis angle, and cine imaging was performed in the range that included the entire left ventricle (Fig.3).

2.3.3 Reduction in imaging time of short-axis image by new method

Five radiologic technologists examined the short-axis image using the new method to find the time required to obtain the short-axis angle and determine whether the respiratory pause time of the subject could be shortened. The time to be considered is the time from the start of imaging of the localized image to

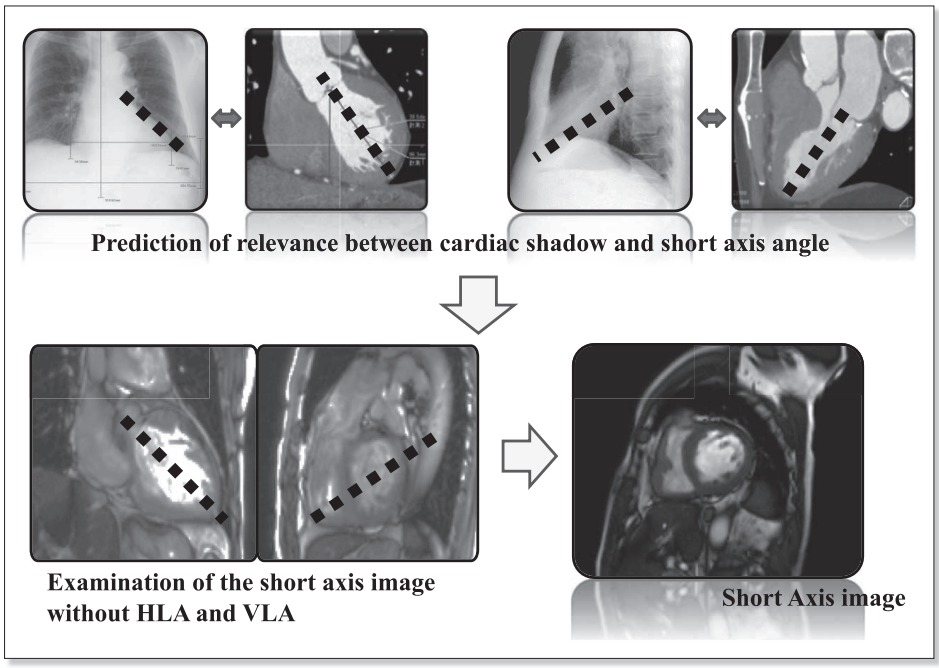

Fig.3 New imaging procedure of short axis imaging

Table 2 Rating criterion for the visual evaluation

Score	Rating criterion
5	No difference compared with the conventional method.
4	Acceptable on diagnosis although an angle may be difference compared with the conventional method.
3	Possibility to affect diagnosis due to a difference short axis angle compared with the conventional method.
2	Unacceptable on diagnosis
1	Not a short axis image

the acquisition of the first short-axis image (the examination time) and the time for which breathing is withheld during the examination (the breath-hold time). The examination time was calculated from Synapse described on the DICOM image, and the breath-hold time was measured using a stopwatch during the examination. Wilcoxon's signed-rank sum test was performed to assess the significant difference.

2.3.4 Comparison of short-axis images

We compared the short-axis image obtained by the conventional method and that captured by the new method. A visual evaluation was performed for comparison using confidence rating by the double blind method.

Two radiologic technologists with experience of 5 to 15 years and two cardiovascular physicians compared the short-axis images of the conventional and the new methods by the double blind method. Using confidence rating as a visual evaluation method, the conventional and new methods were scored based on the rating criterion shown in Table 2. A score was assigned in all cases, and significant difference test was performed using a chi-square test.

3. Result

3.1 Measurement of cardiac short axis in chest X-ray and CT image

3.1.1 Measurement of short-axis angle of heart

In the measurement of the short-axis angle of the heart, the short-axis angle A for all cases was 46.0 ± 11.1°. In addition, the short-axis

Table 3 Measurement of cardiac short axis in chest X-ray and CT image

Measurement angle	Mean (SD)	Median [IQR]	Range
The short-axis angle A	46.0 (11.1)	46.4 [38.6 – 52.4]	21.4 – 72.4
The short-axis supposed angle α	42.6 (10.1)	42.0 [36.0 – 49.8]	18.0 – 69.0
The short-axis angle B	47.6 (7.2)	48.3 [44.0 – 51.8]	27.1 – 73.6
The short-axis supposed angle β	46.8 (6.5)	47.0 [42.5 – 51.0]	27.0 – 65.0

supposed angle α for all cases was 42.6 ± 10.1° on average. The short-axis angle B for all cases was 47.6 ± 7.2°, and the short-axis supposed angle β for all cases was 46.8 ± 6.5° (Table 3).

3.1.2 Relationship between the short-axis angle of the CT and the short-axis assumed angle of the chest X-ray

The relationship between the short-axis angle A and the short-axis supposed angle α is shown in Fig.4. The primary approximation formula was derived as Y=0.94 X+6.13 (Y: cardiac short-axis angle A in the coronal section in the CT image, X: short-axis supposed angle α in the XP front image) and Pearson's correlation coefficient r was 0.85, suggesting a statistically strong correlation. The relationship between the short-axis angle B and the short-axis supposed angle β is shown in Fig.5. The primary approximation formula was derived as Y=0.97 X+1.96 (Y: cardiac short-axis angle B in the sagittal section in the CT image, X: short-axis supposed angle β in the XP lateral image) and Pearson's correlation coefficient r was 0.87, suggesting a statistically strong correlation.

3.1.3 Verification of reproducibility of measurement method

The results of the intra- and inter-reproducibility are shown in Table 4. Regarding the intra-observer reliability of the chest X-ray, the mean difference at the assumed short-axis angle α was −2.15 ± 2.63, and the ICC was 0.91. In addition, the mean difference at the assumed short-axis angle β was −0.90 ± 2.61 with ICC=0.91. Regarding the intra-observer reliability of the CT image, the mean difference at the short-axis angle A was −0.32 ± 2.89, and the ICC was 0.93. The mean difference at the short-axis angle B was −1.03 ± 2.90 with ICC=0.91.

In the inter-observer reliability test of the chest X-ray, the mean difference at the assumed short-axis angle α was −1.75 ± 3.85, and the ICC was 0.82. In addition, the mean difference at the assumed short-axis angle β was 0.15 ± 2.97 with ICC=0.87. In the inter-observer reliability test of the CT, the mean difference at the short-axis angle A was −0.16 ± 4.54, and the ICC was 0.87. In addition, the mean difference at the short-axis angle B was −1.58 ± 2.92 with ICC=0.87.

3.2 Comparison of new and conventional methods

3.2.1 Comparison of imaging time of short-axis image

Comparison of the examination time in each method is shown in Fig.6 and the comparison of the breath-holding time is shown in Fig.7. The examination time in the conventional method was 619.4 ± 215.6 s and the breath-holding time was 122.0 ± 15.4 s. In comparison, the examination time in the new method was 76.4 ± 9.6 s ($p<0.05$ in comparison with the conventional method) and the breath-holding time was 18.6 ± 0.9 s ($p<0.05$ in

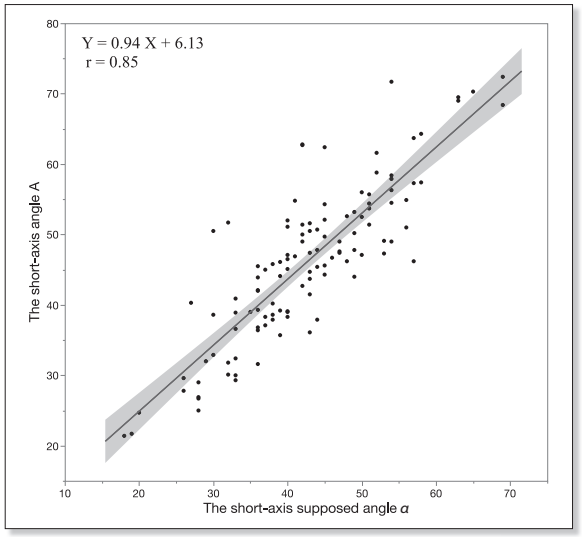

Fig.4 The relationship between the short-axis angle A and the short-axis supposed angle α

The primary approximation formula was derived as Y=0.94 X+6.13 (Y: cardiac short-axis angle A in the coronal section in the CT image, X: short-axis supposed angle α in the XP front image) and Pearson's correlation coefficient r was 0.85, suggesting a statistically strong correlation.

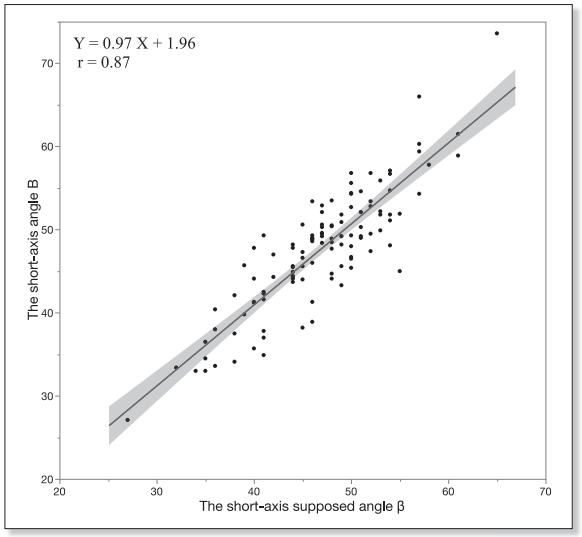

Fig.5 The relationship between the short-axis angle B and the short-axis supposed angle β

The primary approximation formula was derived as Y=0.97 X+1.96 (Y: cardiac short-axis angle B in the sagittal section in the CT image, X: short-axis supposed angle β in the XP lateral image) and Pearson's correlation coefficient r was 0.87, suggesting a statistically strong correlation.

Table 4　The assessment of reproducibility for the measurement of the short axis angle

Intra-observer reliability

Parameters	Analysis 1	Analysis 2	Mean Difference	ICC
The assumed short-axis angle α	43.4 ± 8.66	41.3 ± 9.41	-2.15 ± 2.63	0.91*
The assumed short-axis angle β	46.8 ± 6.58	45.9 ± 6.61	-0.90 ± 2.61	0.91*
The short-axis angle A	44.0 ± 9.71	43.7 ± 9.06	-0.32 ± 2.89	0.93*
The short-axis angle B	46.1 ± 7.11	45.0 ± 8.27	-1.03 ± 2.90	0.91*

Inter-observer reliability

Parameters	Observer 1	Observer 2	Mean Difference	ICC
The assumed short-axis angle α	43.4 ± 8.66	41.7 ± 8.27	-1.75 ± 3.85	0.82*
The assumed short-axis angle β	46.8 ± 6.58	47.0 ± 4.60	0.15 ± 2.97	0.83*
The short-axis angle A	44.0 ± 9.71	43.9 ± 9.35	-0.16 ± 4.54	0.87*
The short-axis angle B	46.1 ± 7.11	44.5 ± 6.05	-1.58 ± 2.92	0.87*

*Value are Mean ± SD, SD: standard deviation, ICC: intraclass correlation coefficient. *=p<0.05.*

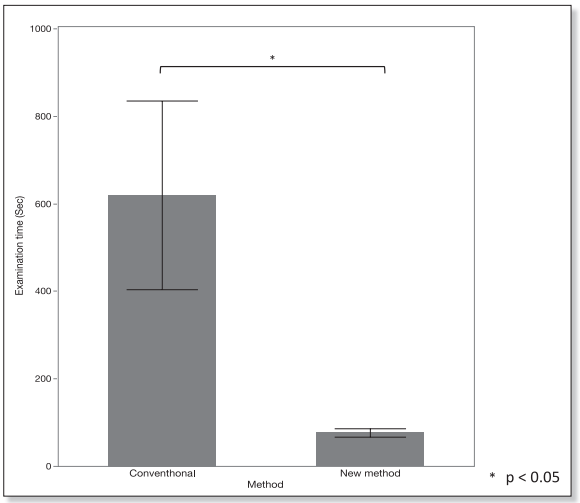

Fig.6　Comparison of the examination time in each method

The Boxes show the mean value, with whiskers indicate standard deviation. *=p<0.05.
The examination time in the new method was 76.4±9.6 s although the conventional method was 619.4±215.6 s (p<0.05).

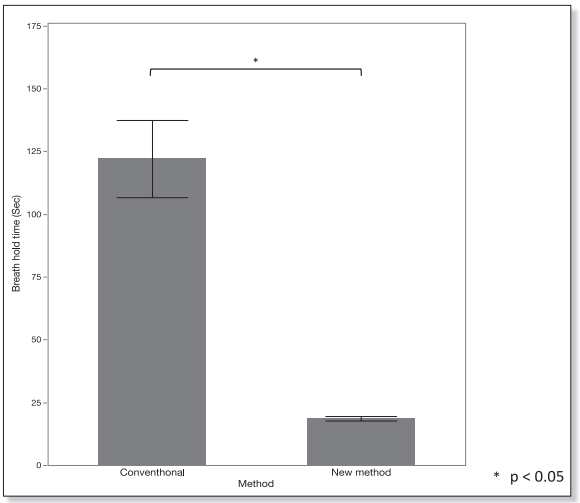

Fig.7　Comparison of the breath-holding time in each method

The Boxes show the mean value, with whiskers indicate standard deviation. *=p<0.05.
The examination time in the new method was 18.6±0.9 s although the conventional method was 122.0±15.4 s (p<0.05).

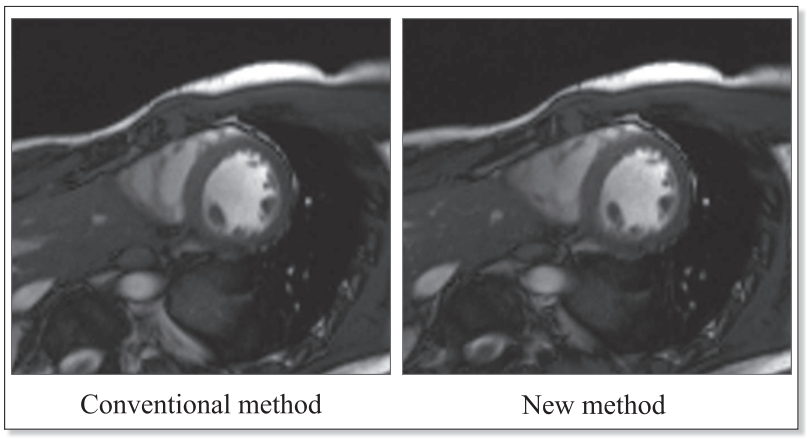

Fig.8　Examples of short-axis images with the conventional and the new methods

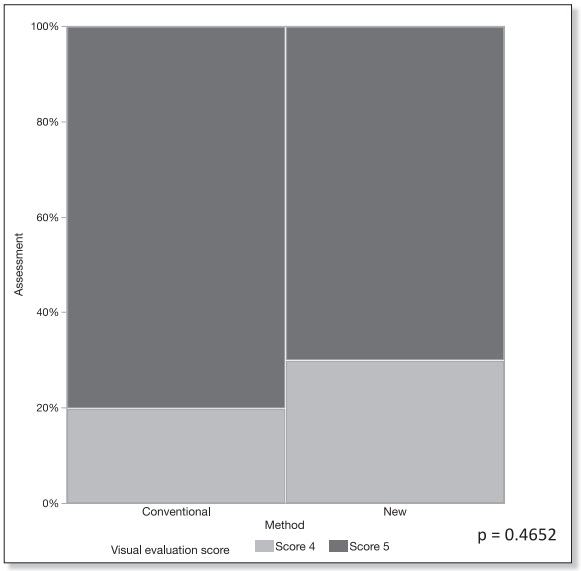

Fig.9 The results of the visual evaluations of the short-axis image by the conventional and the new methods

The average of the confidence rating method scores was 4.8±0.4 points in the conventional method and 4.7 ±0.4 points in the new method. No significant difference was observed between the conventional method and the new method in the chi-square test for visual evaluation (p=0.4652).

comparison with the conventional method).

3.2.2 Comparison of short-axis images

Examples of short-axis images with the conventional and the new methods are shown in Fig.8. Furthermore, the results of the visual evaluations of the short-axis image by the conventional and the new methods are shown in Fig.9. In the visual evaluation, the average of the confidence rating method scores was 4.8 ± 0.4 points in the conventional method and 4.7 ± 0.4 points in the new method. In the new method, one observer assigned 5 points to all cases, and the lowest score assigned by all observers was 4 points. In the result of the chi-square test for visual evaluation, no significant difference was observed between the conventional method and the new method ($p=0.47$).

4. Discussion

In this study, it was suggested that it is possible to estimate the cardiac short axis from the cardiac shadow by clarifying the relationship between the cardiac shadow of the chest X-ray image and the short axis of the heart. Presently, a standardization protocol for cardiac MRI examination has been published by the Society of Cardiovascular Magnetic Resonance (SCMR) [9]. According to this protocol, the scout images of the body axis of the axial, coronal, and lateral views are first examined to assess the position of the heart. Thereafter, the image sections of the HLA and VLA are set by acquiring a cross-sectional image across the body axis covering the entire chest. This protocol consumes considerable examination and breath-hold time for obtaining the short-axis image, which can be painful for the patient. In this study, the angles of the outermost edges of the third and fourth bows of the cardiac shadow in the XP frontal view were used as the determining index of the angle of the left ventricle. The third bow of the cardiac shadow shows the left atrium from the anatomical positional relationship and the fourth bow of the cardiac shadow shows the left ventricle[10]. Therefore, we could estimate the possibility of predicting the short axis of the heart from the cardiac shadow by estimating that the extracardiac lateral side is the angle formed by the left atrium and the left ventricle.

Several outliers are seen in the relation between the short-axis supposed angle α and the cardiac short-axis angle A. These cases corresponded to patients with dilated cardiomyopathy, cardiac tumor, and pericardial effusion, and they are believed to be due to the change in the cardiac shadow in the X-ray frontal image.

Furthermore, in the XP lateral image, the point at the back of the cardiac shadow is used as the indicator, which can be determined on the position of the left atrium and on the image. This index can be measured without being affected by the cardiac shadow even in the above-mentioned case; therefore, it can be concluded that a very strong correlation was obtained.

We also evaluated the intra- and inter-reproducibility to assess the reliability of these analyses. We could confirm high measurement reliability in each analysis. The inter-observer reproducibility in the short-axis supposed angle α of the XP frontal image was less than the maximum reproducibility. This may be due to a slight mismatch between analysis of the starting point and ending point positions of the cardiac shadow in the third and fourth bows, which are the measurement indexes. However, the analysis method is considered very reliable because the mean difference between each observer was -1.75 ± 3.85 degrees and the ICC was 0.82 from the statistical evaluation. This is despite the fact that the definitions of the starting points of the third bow and the fourth bow were ambiguous, as the measurement part uses a clearly identifiable index as the outer side edge.

With the proposed method, it is possible to obtain a short-axis image without HLA

and VLA imaging. Therefore, it is understood that it is possible to drastically reduce the examination time and number of breath-holds until the acquisition of the short-axis image. In the conventional method, the examination time until the acquisition of the short-axis image varied widely (Fig.6). This may be because of the necessity to examine the localizer multiple times and because of the variation in the operator settings. On the other hand, the operator-induced variation in the examination time in the new method remarkably decreased. Moreover, the duration from the imaging of the localizer until the imaging of the short-axis image is minimized, and the setting time for the short-axis image is reduced. Because the angle of the imaging section in the new method is derived by the shape of the heart of the subject, almost no change in the imaging cross section occurs due to the difference in the operator. Therefore, even if a follow-up examination is required, it is possible to provide images with high repeatability of past short-axis cross sections of the heart. As an additional study, the differences in the imaging angle in the coronal and sagittal sections in cardiac MRI images with respect to the body axis when imaging with the new method and the conventional method were compared. The difference in the angle in the coronal section was 90.8 ± 3.5°, and that in the sagittal section was 91.0 ± 3.7°, which indicates that approximately the same angle was obtained in each method. The results of the visual evaluation suggested that there was no influence of this angle difference. In addition, the new method has the ability to image the VLA and HLA after obtaining the short-axis image. In the conventional method, the short-axis image is obtained after imaging the VLA and HLA. However, in this new method, it is possible to freely determine the imaging section after operating the localizer.

Several comparable research reports have reported techniques for detecting the short axis of the heart. Nitta, et al. [11] published an application technology to detect the cardiac reference cross section using the body-axis transverse plane covering the entire heart. Clare E. Jackson, et al. [12] estimated the angle of the cardiac short axis using the threshold of the signal value of the image. However, these prior studies used special application software or algorithms, and have the disadvantage that it is difficult to easily adopt these techniques. Also, in recent years, compressed sensing technology has been noted as a high-speed MRI imaging technology [13].

Compressed sensing refers to a group of methods for accelerated MR data acquisition based on semi-random, incomplete sampling of k-space. A final image is created through an iterative optimization process using non-Fourier transformation and thresholding of intermediately reconstructed images. Recently, some MRI devices can use compressed sensing technology and it has ability to reduce the imaging time significantly. However, it is still in the development stage and there are a lot of MRI devices without this technology. In this research, we established a method to estimate the short-axis cross section without special application software or complicated algorithms. This will encourage its adoption in more facilities.

We need to state the limitations of this research. First, because this is a cross-sectional study and does not have the concept of elapsed time, it does not consider the change in the medical condition over time. Therefore, the proposed method may be unusable if there is a sudden change in the medical condition during the period between cardiac MRI and chest X-ray imaging.

Next, a difference in the examination positions arises, as the chest X-ray is taken in the standing position whereas the cardiac CT is taken in the supine position. Although the relationships between these images were statistically strongly correlated in this study, it is necessary to pay attention to the difference in the examination positions, as it has been reported that a change in the examination position affects the visualization of the cardiac shadow in the chest X-ray image [14]. Nevertheless, the new method of imaging proposed in this study makes it possible to set a short-axis cross section by using the outermost edges of the heart at the time of cardiac MRI. Therefore, it would be unnecessary to consider the examination position.

At last, there is a difference of the type of participants between CCTA and MRI in this study. While CT scans often predominantly complained of coronary artery disease, MRI scans often targeted patients with cardiomyopathy or arrhythmias. Unfortunately, all participants who underwent MRI in this study were normal volunteers. This must be considered as a limitation of this study. However, we believe that this can be useable for more cases in this new method because the present study indicate that the indices of the cardiac short axis and cardiac shadow are almost same unless affected by a cardiac tumor or the like.

5. Conclusion

In this study, we devised a method to image the cardiac short axis without VLA and HLA.

It was demonstrated that the new method could shorten the examination and breath-hold time of the patient. In addition, it provides highly reproducible images irrespective of the operator-induced variation.

Acknowledgments

The authors are grateful to all staff of the Department of Radiological Technology, Showa University Hospital, for their cooperation in this study. This manuscript was partly supported by Akiyoshi Ohtsuka Fellowship of the Japanese Society of Radiological Technology for improvement in English expression of a draft version of the manuscript. We would like to thank Editage (www.editage.jp) for English language editing.

Funding: No funding was received for this study

Compliance with Ethical Standards: All procedures performed in the study that involved human participants were in accordance with the ethical standards of the Ethics Committee at the Showa University School of Medicine and with the 1964 Helsinki declaration and its later amendments or comparable ethical standards. As an animal rights disclosure statement, this article does not contain any studies with animals performed by any of the authors.

Informed Consent: Informed consent was obtained from all individual participants included in the study.

Conflicts of Interest: The authors declare that they have no conflict of interest.

References

1) Kwong RY, et al.: Impact of unrecognized myocardial scar detected by cardiac magnetic resonance imaging on event-free survival in patients presenting with signs or symptoms of coronary artery disease. Circulation, 113: 2733-43, 2006.
2) Lund GK, et al.: Prediction of left ventricular remodeling and analysis of infarct resorption in patients with reperfused myocardial infarcts by using contrast-enhanced MR imaging. Radiology, 245: 95-102, 2007.
3) Larose E, et al.: Right ventricular dysfunction assessed by cardiovascular magnetic resonance imaging predicts poor prognosis late after myocardial infarction. J. Am. Coll. Cardiol., 49: 855-62, 2007.
4) Ebeling Barbier C, et al.: Clinically unrecognized myocardial infarction detected at MR imaging may not be associated with atherosclerosis. Radiology, 245: 103-10, 2007.
5) Schwitter J, et al.: MR-IMPACT: comparison of perfusion-cardiac magnetic resonance with single-photon emission computed tomography for the detection of coronary artery disease in a multicentre, multivendor, randomized trial. Eur. Heart J., 29: 480-9, 2008.
6) Niemann PS, et al.: Anatomically oriented right ventricular volume measurements with dynamic three-dimensional echocardiography validated by 3-Tesla magnetic resonance imaging. J. Am. Coll. Cardiol., 50: 1668-76, 2007.
7) Sakuma H, et al.: Evaluation of left ventricular volume and mass with breath-hold cine MR imaging. Radiology, 188: 377-80, 1993.
8) Grothues F, et al.: Comparison of interstudy reproducibility of cardiovascular magnetic resonance with two-dimensional echocardiography in normal subjects and in patients with heart failure or left ventricular hypertrophy. Am. J. Cardiol., 90: 29-34, 2002.
9) Kramer CM, et al.: Standardized cardiovascular magnetic resonance (CMR) protocols 2013 update. J. Cardiovasc. Magn. Reson., 15: 91, 2013.
10) Anderson RH, et al.: Cardiac anatomy revisited. J. Anat., 205: 159-77, 2004.
11) Nitta S, et al.: Automatic slice alignment method for cardiac magnetic resonance imaging. MAGMA, 26: 451-61, 2013.
12) Jackson CE, et al.: Computerized planning of the acquisition of cardiac MR images. Comput. Med. Imaging Graph., 28: 411-8, 2004.
13) Lustig M, et al.: Compressed Sensing MRI. IEEE Signal Processing Magazine, 25: 72-82, 2008.
14) Funahiki T: Adaptation and limitation of simple X-ray examination. Medicina, 54: 626-9, 2017. (in Japanese)